

Loss-based prior for the degrees of freedom of the Wishart distribution

Sotiris Prevenas* Rachel McCrea[†] Luca Rossini[‡] Cristiano Villa[§]

December 24, 2024

Abstract

In this paper we propose a novel method to deal with Vector Autoregressive models, when the Normal-Wishart prior is considered. In particular, we depart from the current approach of setting $\nu = m + 1$ by setting a loss-based prior on ν . Doing so, we have been able to exploit any information about ν in the data and achieve better predictive performances than the method currently used in the literature. We show how this works both on simulated and real data sets where, in the latter case, we used data of macroeconomic fashion as well as viral data. In addition, we show the reason why we believe we achieve a better performance by showing that the data appears to suggest a value of ν far from the canonical $m + 1$ value.

Keyword: Forecasting, Loss-based prior, Normal-Wishart prior, Vector Autoregressive models

1 Introduction

Vector autoregressive (VAR) models are widely used by macroeconomists and central bankers for analysing and forecasting time series related to finance or economic problems. In particular, VAR models are flexible multivariate time series that capture interdependencies among multiple variables of interest. They have been introduced in [Sims \(1980\)](#) and recently have been used to analyse dynamic properties of economic variables.

In order to avoid overparametrization and overfitting issues, Bayesian inference for VAR models has been successfully introduced (e.g. [Doan et al., 1984](#); [Litterman, 1986](#); [Sims and Zha, 1998](#)). In the recent literature, different prior specifications for the matrix of coefficients of the VAR models have been developed. In particular, [Doan et al. \(1984\)](#) and [Litterman \(1986\)](#) have introduced a set of prior distributions that center the whole system on a multivariate random walk. In order to deal with high dimensional models and forecasting of macroeconomic scenarios (e.g. [Bańbura et al., 2010](#); [Carriero et al., 2015, 2019](#); [Huber and Feldkircher, 2019](#)), hierarchical models have been introduced to deal with dimensionality issues. For instance, [George et al. \(2008\)](#) introduced stochastic search variable selection (SSVS) priors, while recently different papers show improvements in inference and forecasting when dealing with parametric

*University of Kent, United Kingdom. sp798@kent.ac.uk

[†]University of Kent, United Kingdom. r.s.mccrea@kent.ac.uk

[‡]Queen Mary University of London, United Kingdom. 1.rossini@qmul.ac.uk

[§]Newcastle University, United Kingdom. cristiano.villa@ncl.ac.uk

(e.g., Normal Gamma or Dirichlet Laplace, see [Huber and Feldkircher \(2019\)](#) and [Cross et al. \(2020\)](#)) and nonparametric (see Bayesian additive regression trees (BART), see [Huber and Rossini \(2020\)](#), and Dirichlet process, see [Billio et al. \(2019\)](#)) shrinkage priors.

In case of constant volatility models, all the approaches previously described deal with Wishart prior distributions for the variance-covariance matrix. Thus, the most common specifications of the prior for the VAR is the Normal-Wishart distributions, where the matrix of coefficients follows a-priori a Normal distribution and the covariance matrix a Wishart distribution. The nice follow up of this representation is the possibility of having closed-form posterior distributions, which moves in the same way as the prior specification.

In the usual representation of the Wishart distribution, we are inferring the degree of freedom and the scale matrix. In particular, in the VAR representation, the degrees of freedom are assumed a-priori to be equal to the size of the variable of interest plus one. As far as we are aware, no investigation has been done regarding this assumption and in this paper, we address with this issue. In particular, we assume an hyper-prior for the degrees of freedom by following the literature on loss-based priors (see [Villa and Walker, 2015](#)).

As stated in the simulation and empirical studies, the use of an hyper-prior on the degrees of freedom leads to better results with respect to fixing a-priori the value of the degrees of freedom. This result provides the opportunity to investigate different values of the degrees of freedom. The aim of this paper is to contribute to the literature on multivariate time series by introducing a novel hyper-prior on the degree of freedom.

We illustrate the better performance of our hyper-prior with respect to fixing the degrees of freedom by applying our approach to two different datasets. In the first application, to assess how our model performs in a typical real-data application, we forecast different macroeconomic variables in the US by using FRED dataset ([McCracken and Ng, 2020](#)). We study the merits of our approach by considering three datasets of differing size, namely, a small (with $m = 3$), a medium (with $m = 7$) and a large (with $m = 15$) dataset. The second dataset analysed is the Google Dengue Trends (GDT) for ten different countries ([Carneiro and Mylonakis, 2009](#); [Strauss et al., 2017](#)). In both applications, we perform out-of-sample measures to measure the forecasting accuracy of our approach with respect to the Normal-Wishart prior. Comparing the two models reveals that our approach improves in terms of root mean square errors (RMSE) and continuous rank probability scores (CRPS).

The article is organized as follows. Section 2 described the VAR model and the usual Normal-Wishart prior setup. Section 3 focuses on the derivation of the loss-based prior for the degrees of freedom of the Wishart distribution. In Section 4, we compare the proposed hyper-prior with the benchmark assumption using data simulated from a multivariate time series. Section 5 deals with real data, in particular we forecast macro-economic and Google dengue trends data. Final discussion points and conclusions are presented in Section 6.

2 Preliminaries

Let \mathbf{y}_t for $t = 1, \dots, T$ be the m -dimensional vector of observations, then we can define a VAR model with p lags as

$$\mathbf{y}_t = \sum_{j=1}^p A_j \mathbf{y}_{t-j} + \boldsymbol{\varepsilon}_t, \quad (1)$$

where A_j is a $(m \times m)$ matrix of coefficients and $\boldsymbol{\varepsilon}$ an m -dimensional vector of errors. We assume that $\boldsymbol{\varepsilon}_t = (\varepsilon_{1t}, \dots, \varepsilon_{mt})$ are i.i.d. for $t = 1, \dots, T$ with Gaussian distribution $\mathcal{N}(0, \Sigma)$.

Eq. (1) can be written in the more compact form as

$$Y = XA + E,$$

where Y is a $T \times m$ matrix constructed as $Y = (\mathbf{y}_1, \mathbf{y}_2, \dots, \mathbf{y}_T)'$, X is a $T \times k$ matrix constructed as $X = (\mathbf{x}_1, \mathbf{x}_2, \dots, \mathbf{x}_T)'$ where $\mathbf{x}_t = (\mathbf{y}'_{t-1}, \mathbf{y}'_{t-2}, \dots, \mathbf{y}'_{t-p})$ and contains the lagged response variables. Moreover, A is a $k \times m$ matrix of coefficients constructed as $A = (A_1, A_2, \dots, A_p)$ and E is a $T \times m$ matrix of errors constructed as $E = (\boldsymbol{\varepsilon}_1, \dots, \boldsymbol{\varepsilon}_T)'$. As a further step, we can define the VAR models of order p in a vectorized form

$$\mathbf{y} = (I_m \otimes X) \boldsymbol{\alpha} + \boldsymbol{\varepsilon},$$

where $\mathbf{y} = \text{vec}(Y)$, $\boldsymbol{\alpha} = \text{vec}(A)$ and $\boldsymbol{\varepsilon} = \text{vec}(E)$ with distribution $\boldsymbol{\varepsilon} \sim \mathcal{N}(0, \Sigma \otimes I_T)$ and \otimes is the Kronecker product.

In this paper, we adopt a Normal-Wishart prior for the parameters of the model, where we assume a Normal prior distribution for the matrix of coefficients such as $\boldsymbol{\alpha} \sim \mathcal{N}(\underline{\boldsymbol{\alpha}}, \underline{V})$. On the other hand, we assume a Wishart distribution for the precision matrix $\Sigma^{-1} \sim \mathcal{W}(\underline{\nu}, \underline{S}^{-1})$.

The nice property of the Normal-Wishart prior is the possibility to have a conditional posterior distribution for the parameters in the closed form, which follows the same distribution as the prior assumptions. In particular, the posterior distribution of the vectorized matrix of coefficients is

$$\boldsymbol{\alpha} | \mathbf{y}, \Sigma^{-1} \sim \mathcal{N}(\bar{\boldsymbol{\alpha}}, \bar{V}),$$

where $\bar{V} = (\underline{V}^{-1} + \sum_{t=1}^T Z_t' \Sigma^{-1} Z_t)^{-1}$ and $\bar{\boldsymbol{\alpha}} = \bar{V} \left(\underline{V}^{-1} \underline{\boldsymbol{\alpha}} + \sum_{t=1}^T Z_t' \Sigma^{-1} \mathbf{y}_t \right)$, where $Z_t = (I_m \otimes X_t)$. On the other hand, the posterior distribution for the precision matrix is

$$\Sigma^{-1} | \boldsymbol{\alpha}, \mathbf{y} \sim \mathcal{W} \left(\bar{\nu}, \bar{S}^{-1} \right),$$

where $\bar{\nu} = \underline{\nu} + T$ and $\bar{S} = \underline{S} + \sum_{t=1}^T (\mathbf{y}_t - Z_t \boldsymbol{\alpha})(\mathbf{y}_t - Z_t \boldsymbol{\alpha})'$.

3 Loss-based hyperprior

In this Section we derive the loss-based prior distribution for the number of degrees of freedom of the Wishart distribution. We consider the parameter ν as discrete and, to construct the prior, we employ the objective method introduced in [Villa and Walker \(2015\)](#).

To illustrate the method, let us consider a Bayesian model with sampling distribution $f(x|\theta)$, characterized by the discrete parameter $\theta \in \Theta$, and prior $\pi(\theta)$. The idea is to assign a mass to each value of the parameter that is proportional to the Kullback–Leibler divergence between the model defined by θ and the nearest one. In other words, if $f(x|\theta)$ is the true model, and it is not chosen, then the loss in information that one would incur is represented by the Kullback–Leibler divergence from $f(x|\theta)$ and $f(x|\theta')$, where the latter is the nearest model to the true one. Thus, the prior on θ , will be given by Eq. (2).

$$\pi(\theta) \propto \exp \left\{ \min_{\theta' \neq \theta \in \Theta} KL(f(x|\theta) \| f(x|\theta')) \right\} - 1, \quad (2)$$

where $KL(f(x|\theta) \| f(x|\theta'))$ represents the Kullback–Leibler divergence between the two models.

In order to derive the prior in Eq. (2) for ν , we need to obtain the Kullback–Leibler divergence between two Wishart distributions that share the same scale matrix V and differ in the number of degrees of freedom only. The probability density function of a Wishart with parameters V and ν is given by:

$$W(X|V, \nu) = \frac{|X|^{(\nu-m-1)/2} \exp(-\text{Tr}(V^{-1}X)/2)}{2^{\frac{\nu m}{2}} |V|^{\nu/2} \Gamma_m(\nu/2)},$$

where $\Gamma_m(\cdot)$ is the multivariate Gamma function, and $\text{Tr}(\cdot)$ is the trace function. Thus the Kullback–Leibler divergence between two Wishart distributions that differ only in the number of degrees of freedom, say W_ν and $W_{\nu+c}$, is given by:

$$KL(W_\nu \| W_{\nu+c}) = \log \left\{ \frac{\Gamma_m(\frac{\nu+c}{2})}{\Gamma_m(\frac{\nu}{2})} \right\} - \frac{c}{2} \psi_m \left(\frac{\nu}{2} \right),$$

where ψ_m is the multivariate digamma function defined as $\psi_m(x) = \sum_{i=1}^m \psi(x + (1-i)/2)$, $\psi(x) = \Gamma'(x)/\Gamma(x)$ is the digamma function and $c \in \mathbb{Z}$. As $KL(W_\nu \| W_{\nu+c})$ is a convex function of c , and its global minimum is at $c = 0$, the nearest Wishart distribution to W_ν will be $W_{\nu+c}$ for either $c = -1$ or $c = 1$. The following Theorem 1 shows that the Kullback–Leibler divergence between W_ν and $W_{\nu+c}$ is minimized for $c = 1$.

Theorem 1. *Consider two Wishart distributions, W_ν and $W_{\nu+c}$, with the same scale matrix, with ν and $\nu+c$ degrees of freedom, respectively, and where $c \neq 0$ is an integer. The Kullback–Leibler divergence between W_ν and $W_{\nu+c}$ is minimum for $c = 1$.*

Proof. For $c = 1$, the Kullback–Leibler divergence is

$$KL(W_\nu \| W_{\nu+1}) = \log \Gamma_m \left(\frac{\nu+1}{2} \right) - \log \Gamma_m \left(\frac{\nu}{2} \right) - \frac{1}{2} \psi_m \left(\frac{\nu}{2} \right),$$

and for $c = -1$, we have

$$KL(W_\nu \| W_{\nu-1}) = \log \Gamma_m \left(\frac{\nu-1}{2} \right) - \log \Gamma_m \left(\frac{\nu}{2} \right) + \frac{1}{2} \psi_m \left(\frac{\nu}{2} \right).$$

By taking the difference of the two divergences, we have

$$\begin{aligned} KL(W_\nu \| W_{\nu+1}) - KL(W_\nu \| W_{\nu-1}) &= \log \Gamma_m \left(\frac{\nu+1}{2} \right) - \log \Gamma_m \left(\frac{\nu-1}{2} \right) - \psi_m \left(\frac{\nu}{2} \right) \\ &= \log \frac{\Gamma(\nu)}{2^m \Gamma(\nu - m)} - \psi_m \left(\frac{\nu}{2} \right). \end{aligned}$$

We will prove that this difference is always negative for any ν, m such that $\nu > m \geq 2$. As $\nu > m$ it is of the form $\nu = m + k$, $k = 1, 2, \dots, m \geq 2$. By proving the following inequality we prove that the minimum Kullback–Leibler divergence is achieved at $c = 1$.

$$\log \left\{ \frac{\Gamma(m+k)}{2^m \Gamma(k)} \right\} < \psi_m \left(\frac{m+k}{2} \right). \quad (3)$$

Two results that enable us to prove the inequality in (3), are the following:

$$\psi_{m+1} \left(\frac{\nu+1}{2} \right) = \psi_m \left(\frac{\nu}{2} \right) + \psi \left(\frac{\nu+1}{2} \right), \quad (4)$$

and

$$\log \left(x - \frac{1}{2} \right) < \psi(x). \quad (5)$$

Eq. (4) comes from the definition of the multivariate digamma function, and inequality (5) can be deduced from the inequality $\log(x + \frac{1}{2}) - \frac{1}{x} < \psi(x) < \log(x + e^{-\gamma}) - \frac{1}{x}$, (see [Elezovic et al., 2000](#)) for $x > \frac{1}{2}$ and with γ equal to 0.57721, the Euler–Mascheroni constant.

At first, we make the assumption that it holds for a particular m and prove that it holds for $m + 1$.

$$\begin{aligned} \log \left\{ \frac{\Gamma(m+1+k)}{2^{m+1} \Gamma(k)} \right\} &< \psi_{m+1} \left(\frac{m+1+k}{2} \right) \\ \log \left\{ \frac{\Gamma(m+k)(p+k)}{2^m \Gamma(k) 2} \right\} &< \psi_m \left(\frac{m+k}{2} \right) + \psi \left(\frac{m+1+k}{2} \right) \\ \log \left\{ \frac{\Gamma(m+k)}{2^m \Gamma(k)} \right\} + \log \left\{ \frac{m+k}{2} \right\} &< \psi_m \left(\frac{m+k}{2} \right) + \psi \left(\frac{m+1+k}{2} \right), \end{aligned}$$

where in the last step we have $\log \frac{m+k}{2} < \psi \left(\frac{m+1+k}{2} \right)$ as a consequence of the result in (5).

Thus, if the inequality (3) holds for m , then it holds for $m + 1$ and, more importantly, it holds for any k . The smallest value m can have is $m = 2$, for which we have

$$\begin{aligned}\log \left\{ \frac{\Gamma(2+k)}{2^2 \Gamma(k)} \right\} &< \psi_2 \left(\frac{2+k}{2} \right) \\ \log \left\{ \frac{(k+1)k}{2^2} \right\} &< \psi \left(\frac{2+k}{2} \right) + \psi \left(\frac{1+k}{2} \right).\end{aligned}$$

But again, we have $\log \left(\frac{k}{2} \right) < \psi \left(\frac{k+1}{2} \right)$ and $\log \left(\frac{k+1}{2} \right) < \psi \left(\frac{k+2}{2} \right)$ due to (5). So inequality (3) holds for $m = 2$ and, subsequently, it holds for any m . \square

Now we can define the objective prior distribution for ν , following Eq. (2), as

$$\pi(\nu) \propto \frac{\Gamma \left(\frac{\nu+1}{2} \right)}{\Gamma \left(\frac{\nu+1-m}{2} \right)} e^{-\frac{1}{2} \sum_{i=1}^m \psi \left(\frac{\nu+1-i}{2} \right)} - 1. \quad (6)$$

3.1 Properness of the posterior for ν

Let us assume that we observe one random matrix Σ^{-1} from the Wishart $W(S_0^{-1}, \nu)$. Thus, the likelihood function will have the following form

$$\begin{aligned}p(y|\alpha, \Sigma) &= (2\pi)^{-\frac{mT}{2}} |\Sigma|^{-\frac{T}{2}} \exp \left\{ -\frac{1}{2} [y - (I_m \otimes X)\alpha]' (\Sigma^{-1} \otimes I_T) [y - (I_m \otimes X)\alpha] \right\} \\ &\propto |\Sigma|^{-\frac{T}{2}} \exp \left\{ -\frac{1}{2} \text{Tr} [(Y - XA)' (Y - XA) \Sigma^{-1}] \right\},\end{aligned} \quad (7)$$

and, using the objective prior for ν in Eq. (2), we obtain the following posterior distribution for the number of degrees of freedom:

$$\begin{aligned}p(\nu|\Sigma^{-1}) &\propto \pi(\nu) \pi \left(\Sigma^{-1} | \nu, S_0^{-1} \right) \\ &\propto \left\{ \frac{\Gamma \left(\frac{\nu+1}{2} \right)}{\Gamma \left(\frac{\nu+1-m}{2} \right)} e^{-\frac{1}{2} \sum_{i=1}^m \psi \left(\frac{\nu+1-i}{2} \right)} - 1 \right\} \left\{ \frac{|\Sigma^{-1}|^{(\nu-m-1)/2} e^{(-\text{Tr}(S_0 \Sigma^{-1})/2)}}{2^{\frac{\nu m}{2}} |S_0^{-1}|^{\nu/2} \Gamma_m \left(\frac{\nu}{2} \right)} \right\}.\end{aligned} \quad (8)$$

An important aspect when using an objective prior, is to ensure that the yielded posterior is proper. The following Theorem 2 shows that the marginal posterior for ν is proper.

Theorem 2. *The posterior distribution for the number of degrees of freedom ν in Eq. (8) is proper.*

Proof. We prove that $\sum_{\nu=m}^{\infty} p(\nu|\Sigma^{-1}) < \infty$ using Abel's test of convergence. The sequence $\{\pi(\nu)\}$ is bounded : $\pi(m) > \pi(\nu) > 0$ and is also monotone (decreasing). We show that

$\sum_{\nu=m}^{\infty} \pi(\Sigma^{-1}|\nu, S_0^{-1}) < \infty$ using the ratio test :

$$\begin{aligned}
R_{\nu} &= \frac{|\Sigma^{-1}|^{(\nu-m)/2}}{2^{\frac{(\nu+1)m}{2}} |S_0^{-1}|^{(\nu+1)/2} \Gamma_m\left(\frac{\nu+1}{2}\right)} \cdot \frac{2^{\frac{\nu m}{2}} |S_0^{-1}|^{\nu/2} \Gamma_m\left(\frac{\nu}{2}\right)}{|\Sigma^{-1}|^{(\nu-m-1)/2}} \\
&= \frac{|\Sigma^{-1}|^{1/2} \Gamma_m\left(\frac{\nu}{2}\right)}{2^{m/2} |S_0^{-1}|^{1/2} \Gamma_m\left(\frac{\nu+1}{2}\right)} \\
&= \frac{|\Sigma^{-1}|^{1/2} \Gamma\left(\frac{\nu+1-m}{2}\right)}{2^{m/2} |S_0^{-1}|^{1/2} \Gamma\left(\frac{\nu+1}{2}\right)}.
\end{aligned}$$

It is that

$$\lim_{\nu \rightarrow \infty} \left\{ \frac{\Gamma\left(\frac{\nu+1-m}{2}\right)}{\Gamma\left(\frac{\nu+1}{2}\right)} \right\} = 0,$$

so $\lim_{\nu \rightarrow \infty} R_{\nu} = 0$ (Abramowitz and Stegun, 1972) and, therefore, the posterior for ν is a proper distribution. \square

4 Simulation Studies

In this section, we compare the performance of our loss-based hyperprior in different simulation studies. In particular, we use a Bayesian Vector autoregressive (VAR) model of order 1 with different matrix dimension and time length. By using this specification, we use two different priors for the covariance matrix, Σ , where in the first scenario we treat the degrees of freedom as fixed at $\nu = m + 1$, and in the second scenario we use our loss-based hyperprior. Regarding the matrix of coefficients in both scenarios, we assume a Normal prior since the interest of our simulation experiment is in the evaluation of the covariance matrix. In formulae, we have that the prior for the matrix of coefficients is a Normal distribution with hyperparameters α_0 and V_0 , while the covariance matrix follows an inverse Wishart with scale matrix equal to S_0 and degrees of freedom equal to $\nu = m + 1$ (in the first scenario) and $\nu \sim \pi(\nu)$ (in the second scenario).

As stated above, we have created different synthetic datasets for various dimension of the matrix in the VAR. In particular, we have studied small, medium and large size VAR, where m is equal to 5, 10 and 20, respectively. For each dataset, we have considered a small time dimension ($T = 30$) and a medium time dimension ($T = 100$).

Moreover, we have considered different combinations for the choice of the degrees of freedom when generating the data. In particular, for each dimension m , we have chosen ν equal to $\{5, 10, 15\}$ for $m = 5$, $\{10, 15, 20\}$ for $m = 10$, and $\{20, 24, 26\}$ for $m = 20$, respectively.

For each dataset, we run the Gibbs sampler that sequentially draws from the conditional posterior distributions $p(\alpha|y, \Sigma^{-1})$, $p(\Sigma^{-1}|y, \alpha)$ for Model 1 and a second Gibbs sampler that draws from $p(\alpha|y, \Sigma^{-1})$, $p(\Sigma^{-1}|y, \alpha)$ and $p(\nu|\Sigma^{-1})^1$ for Model 2. Then, for each posterior

¹In this second scenario, the last posterior distribution is not available in closed-form and thus we need a

sample, we estimate the posterior means of the m^2 coefficients and the elements of Σ and calculate the Root Mean Absolute Deviation between these posterior means and the true parameter values that generated each respective dataset as

$$RMAD = \left[\frac{1}{N} \sum_{i=1}^N |\theta - \hat{\theta}| \right]^{\frac{1}{2}},$$

where N is the number of parameters estimated (which is equal to m^2 for the covariance matrix and depends on the lags for the matrix of coefficients) and θ is the matrix of coefficients or the covariance matrix.

This process is repeated 250 times and the Gibbs sampler is run for 6000 iterations with a burn-in of 1000 iterations. For each batch of Root mean absolute deviations (RMAD), we create different boxplots for the two different scenario, the fixed ν and the estimated degrees of freedom. In particular, since we are interested in the covariance matrix, we have reported the RMADs for the covariance matrices for each dataset. Figure 1 shows the results for the RMAD for the case with $m = 5$ and with $T = 30$ ². In particular, the left panel explains the results when the data are generated with $\nu = 5$, the central panel when the data are generated from $\nu = 10$ and the right panel with $\nu = 15$. From Figure 1, once we move from a dataset generated with a ν equal to m to a dataset with large ν , the differences between the prior increase. In fact, the left panel shows no difference between the two priors, except for the outliers, which are smaller for our proposed hyperprior. On the other hand, increasing the ν to 10 and 15 leads to improvements in the evaluation of our hyperprior. The results are bigger when we evaluate our hyperprior with ν equal to 15 and ν equal to 5.

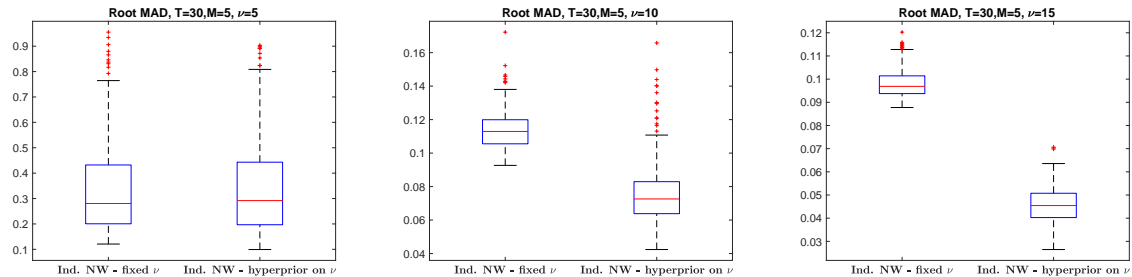


Figure 1: Monte Carlo Simulation - Root Mean Absolute Deviations of the covariance matrices of dimension $m = 5$. These empirical distributions are obtained by simulating 250 VAR(1) of sample size $T = 30$. Results are reported separately for data generated from a Wishart with $\nu = 5$ (left panel); $\nu = 10$ (center panel) and $\nu = 15$ (right panel).

These results are also confirmed in high dimensional cases as shown in Figure 2 and 3 for the ten dimensional and twenty dimensional case, respectively. In Figure 2, we compare our loss-based hyperprior with the fixed ν for the data generated from a Wishart with degrees of freedom equal to 10 (left panel); 15 (center) and 20 (right). As stated above, in this scenario the results state that our loss-based prior is improving with respect to the fixed ν for the case

Metropolis-Hastings step.

²The results for $T = 100$ are available in the Supplementary Material.

of 15 and 20 degrees of freedom. Regarding the smallest degree of freedom, we have small differences between the two prior scenarios, but again the loss-based prior has better results regarding the outlier values.

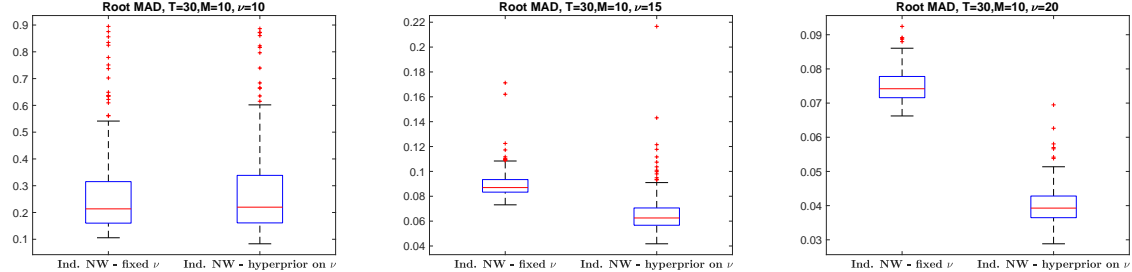


Figure 2: Monte Carlo Simulation - Root Mean Absolute Deviations of the covariance matrices of dimension $m = 10$. These empirical distributions are obtained by simulating 250 VAR(1) of sample size $T = 30$. Results are reported separately for data generated from a Wishart with $\nu = 10$ (left panel); $\nu = 15$ (center panel) and $\nu = 20$ (right panel).

In conclusion, Figure 3 shows the results for the twenty dimensional case. Also in this case, we have reported three different figures for data generated from a Wishart with 20 degrees of freedom (left panel); 24 (center) and 26 (right) with T equal to 30. In this case, the improvements are less evident than the previous case for the left and center panel. However, in the case of 24 degrees of freedom, our loss-based hyperprior outperforms the fixed ν prior. This result is strong when we use data generated from a Wishart with 26 degrees of freedom as stated in the right panel of Figure 3.

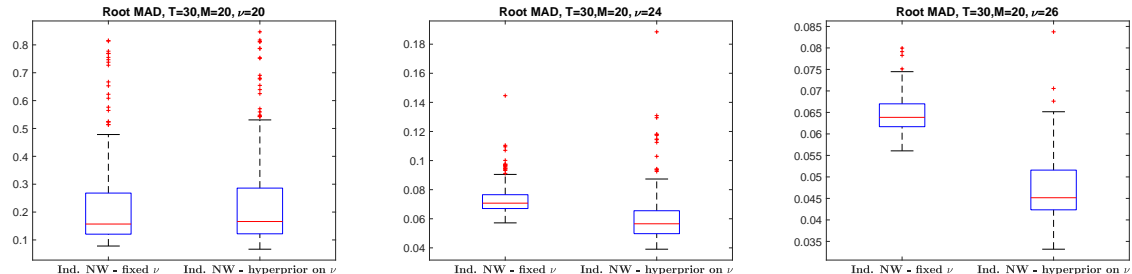


Figure 3: Monte Carlo Simulation - Root Mean Absolute Deviations of the covariance matrices of dimension $m = 20$. These empirical distributions are obtained by simulating 250 VAR(1) of sample size $T = 30$. Results are reported separately for data generated from a Wishart with $\nu = 20$ (left panel); $\nu = 24$ (center panel) and $\nu = 26$ (right panel).

These results are confirmed for a higher number of observations, alias T equal to 100 as shown in the Supplementary material.

5 Forecasting of Real Data

In this section, we compare the results of our loss-based hyperprior with respect to the fixed ν prior by using two different real data applications. The first real data application deals with macroeconomic variables from the FRED dataset and we consider three different sizes: a small

(3 variables), a medium (7 variables) and a large (15 variables) datasets. On the other hand, the second data refers to the Dengue Fever data on 10 different countries across the world.

In both applications, we evaluate the performance of our loss-based hyperprior by forecasting one step ahead values. We compare the predictive ability of the two priors by using a point and a density forecasting. Regarding the point forecasting measure, we use the root mean square error (denoted by RMSE), which is

$$RMSE_i = \left[\frac{1}{T-R} \sum_{t=R}^{T-1} (\hat{y}_{i,t+1} - y_{i,t+1})^2 \right]^{\frac{1}{2}}, \quad (9)$$

where R is the length of the rolling window, $y_{i,t+1}$ the observation for the i variable and $\hat{y}_{i,t+1}$ is the one-step ahead prediction for the i variable.

In addition, we evaluate the density forecasting by the mean of the average continuous ranked probability score (CRPS) introduced by [Gneiting and Raftery \(2007\)](#) and [Gneiting and Ranjan \(2011\)](#). The use of the CRPS has some advantages with respect to the log score since it does a better job of rewarding values from the predictive density that are close to the outcome and it is less sensitive to outlier outcomes. The CRPS is defined such that a lower number is a better score and is given by:

$$\begin{aligned} CRPS_t(y_{t+1}) &= \int_{-\infty}^{+\infty} (F(z) - \mathbb{1}(y_{t+1} \leq z))^2 dz \\ &= E_f |Y_{t+1} - y_{t+1}| - 0.5 E_f |Y_{t+1} - Y'_{t+1}|, \end{aligned} \quad (10)$$

where F is the cumulative distribution function associated with the posterior predictive density, f , $\mathbb{1}(y_{t+1} \leq z)$ is an indicator function taking the value 1 if $y_{t+1} \leq z$ and 0 otherwise, and Y_{t+1} , Y'_{t+1} are independent random draws from the posterior predictive density. For the point and the density forecasting metrics, in the table we show their values and a lower value of the RMSE or of the average CRPS means that the model is forecasting better with respect to the other.

5.1 Macroeconomic Data

The data we used are based on the FRED-QD dataset from [McCracken and Ng \(2020\)](#). The data are on a quarterly frequency and the time period spans from 1959Q2 to 2019Q3. All variables are transformed to be stationary by following [McCracken and Ng \(2020\)](#). In terms of forecasting, this choice leads to more stable predictive densities. Following [Huber and Feldkircher \(2019\)](#), we use three sets of variables to estimate a small-scale, medium-scale and a large-scale VAR. The small-scale VAR only includes the real GDP growth, the GDP deflator and the Federal Funds Rate (FFR). The medium-scale VAR additionally uses data on investment, consumption growth and hours worked. The large-scale VAR includes 15 different variables. Given the quarterly frequency of our data, we include $p = 5$ lags for all the models

considered in this section.

We estimate the models by using the MCMC algorithm and we use 6000 iterations with the first 1000 iterations being discarded. Moreover, regarding the forecasting exercise, we use a rolling window size of 60 quarters and we run one-step ahead forecasts.

Before looking at the forecasting exercise, we briefly show the results of the estimated degrees of freedom by using a rolling window estimation. In particular, we show the results for the three different scales of the posterior mean of the degrees of freedom estimated by using our loss-based hyperprior. Figure 4 shows the results of the estimated degrees of freedom jointly with the 95% highest posterior density (HPD) and the degrees of freedom used in the Normal-Wishart scenario with fixed ν (in red). The left panel shows the results for the small-scale VAR, the center panel for the medium-scale VAR and the right for the large-scale VAR.

In Figure 4, we find strong evidence of changes in the estimated degrees of freedom across the time. Hence, the left panel explains an high jump in the degrees of freedom after the 2000 and a fall around the 2009, strongly related with the Lehman Brothers failure. These results are confirmed also in the medium-scale VAR with an improvement and increase in the last period. These changes are less evident in the large-scale VAR during time, but obviously it provides better results with respect to the fixed ν chosen by the researcher and equal to the number of variables plus one.

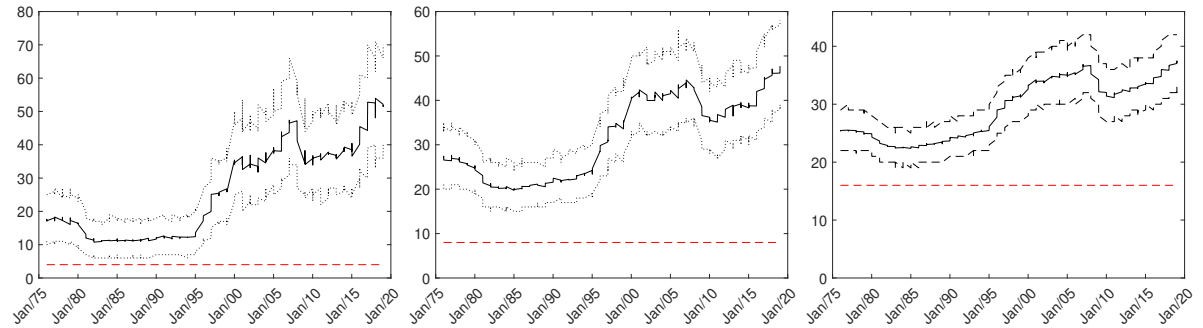


Figure 4: Estimated degrees of freedom (solid line) for the loss based hyperprior by using a rolling window of 60 quarters with the 95% Highest posterior density (dotted lines) and the fixed ν (red dashed line) for the macroeconomic data. Left panel for the small-case; center for the medium-scale and right for the large-scale.

Moving to the forecasting analysis, we have reported the point and density forecasting measures in the same table for the three different cases. Table 1 shows the results for the small-case VAR for the RMSE (left panel) and the CRPS (right panel). In this table, we report the ratio between the two models and when the ratio is less than 1, it means that the model with loss-based hyperprior is outperforming the benchmark model with fixed ν . In the point forecasting measure, the benchmark model is outperforming our hyperprior for the GDP and for the Federal Reserve Fund by a really small quantity, while on the other hand, for the GDP deflator our hyperprior leads to an improvement of around 20% with respect to the benchmark. This result is confirmed for the average CRPS, where our loss-based hyperprior is outperforming of 15% (for the real GDP growth and the GDP deflator) and 2% (for the Federal Reserve Funds Rate) the benchmark model.

	RMSE			CRPS		
	fixed ν	$\nu \sim \pi(\nu)$	ratio	fixed ν	$\nu \sim \pi(\nu)$	ratio
GDPC1	0.010	0.010	1.006	0.045	0.039	0.866
GDPCTPI	0.004	0.003	0.811	0.045	0.039	0.868
FEDFUND	0.946	0.953	1.006	0.388	0.381	0.981

Table 1: RMSE and average CRPS for the small-case VAR for each prior. The first column refers to the variable, the second to the Gibbs sampler with fixed ν and the third with our loss-based hyperprior.

Moving to the medium-scale model, Table 2 presents the point and density measures for the 7 different variables analysed. In this scenario, the situation is similar to the small-case VAR regarding both the point and density forecasting measures. The main change is related to the GDP since the model with hyperprior is outperforming the benchmark of around 5% in point forecasting, while for the Federal Funds Rate, the situation is not changing in point forecasting. As in the small-scale VAR, the average CRPS shows better results with respect to the benchmark model across the 7 variables. In particular, for the three variables of interest, the GDP, GDP deflator and the Federal Funds Rate, the hyperprior model outperforms the benchmark between 3% and 15%. This is also confirmed for the other variables analysed.

	RMSE			CRPS		
	fixed ν	$\nu \sim \pi(\nu)$	ratio	fixed ν	$\nu \sim \pi(\nu)$	ratio
GDPC1	0.008	0.007	0.959	0.058	0.049	0.857
GDPCTPI	0.004	0.004	0.971	0.058	0.050	0.865
FEDFUND	0.941	0.947	1.006	0.391	0.381	0.974
PCECC96	0.006	0.006	1.018	0.058	0.050	0.860
GPDIC1	0.032	0.032	1.003	0.061	0.053	0.866
AWHMAN	0.264	0.260	0.984	0.150	0.144	0.957
CES2000000008x	0.007	0.007	0.909	0.059	0.051	0.859

Table 2: RMSE and average CRPS for the medium-case VAR for each prior. The first column refers to the variable, the second to the Gibbs sampler with fixed ν and the third with our loss-based hyperprior.

In conclusion, we report the results for the large-scale VAR with 15 variables in Table 3. Also in this scenario, the three main variables of interest follow the improvements shown in the medium-scale VAR. In fact, the loss-based hyperprior improves with respect to the benchmark of around 10% for the GDP and its deflator, while for the FFR it is similar from a point forecasting measure. The average CRPS demonstrates that the improvement is stronger for every variable in particular for the FFR. If we look at all 15 variables analysed, the loss-based hyperprior model always outperforms the benchmark in a density forecasting scenario.

5.2 Dengue Data

In the second application, we show the performance of our loss-based hyperprior by using the Google Dengue Trends (GDT). Dengue is a viral infection transmitted by mosquitoes and is in particular present South America and Asia countries. Recently Google has developed a query based reporting system for infectious disease (Carneiro and Mylonakis, 2009; Strauss et al.,

	RMSE			CRPS		
	fixed ν	$\nu \sim \pi(\nu)$	ratio	fixed ν	$\nu \sim \pi(\nu)$	ratio
GDPC1	0.009	0.008	0.910	0.077	0.070	0.913
GDPCTPI	0.005	0.004	0.909	0.078	0.070	0.908
FEDFUNDS	0.949	0.952	1.002	0.397	0.391	0.983
PCECC96	0.007	0.007	0.973	0.078	0.071	0.911
GPDIC1	0.032	0.031	0.984	0.080	0.073	0.914
AWHMAN	0.247	0.246	0.994	0.150	0.144	0.964
CES2000000008x	0.008	0.007	0.880	0.079	0.072	0.906
PRFIx	0.040	0.040	0.999	0.082	0.075	0.916
INDPRO	0.014	0.013	0.908	0.081	0.073	0.905
CUMFNS	1.028	1.018	0.991	0.544	0.533	0.980
SRVPRD	0.007	0.006	0.944	0.081	0.074	0.913
PCECTPI	0.008	0.007	0.904	0.082	0.075	0.912
GPDICTPI	0.007	0.008	1.117	0.082	0.075	0.907
CPIAUCSL	0.009	0.009	1.003	0.083	0.076	0.912
SP500	0.067	0.066	0.993	0.090	0.083	0.919

Table 3: RMSE and average CRPS for the large-case VAR for each prior. The first column refers to the variable, the second to the Gibbs sampler with fixed ν and the third with our loss-based hyperprior.

2017), while previously its accuracy has been assessed for Flu (Davis et al., 2016; Polgreen et al., 2008).

GDT track the Dengue incidence based on internet search patterns and cluster weekly queries for key terms related with the disease. We use GDT data from January 2011 to December 2014 for Argentina, Bolivia, Brazil, India, Indonesia, Mexico, Philippines, Singapore, Thailand and Venezuela, thus having 10 response variables. Following Davis et al. (2016), we examine a vector autoregressive model with two lags and we run a forecasting exercise and we use a rolling window of 104 weekly observations.

Prior to running the forecasting exercise, we have a look at the insample analysis for the ten countries and in particular, we observe the movement of the posterior mean of the degrees of freedom by using our loss-based hyperprior. As stated above, we have run a rolling window estimation and in Figure 5 we report the posterior mean of the degrees of freedom with our hyperprior (solid black line), the 95% HPD in dotted line and the fixed values of ν equal to 11 and used for the estimation of the MCMC algorithm.

Figure 5 shows positive results regarding the rolling window estimation of the degrees of freedom, which is around 20 with respect to the fixed value equal to 11. Furthermore, the estimated degrees of freedom has some movements at the beginning of the sample around 23 and then it decreases and remains stationary.

Moving to the forecasting exercise, we evaluate the forecasting by using a point and a density forecasting measure. Table 4 shows the results for each country and except for Argentina, for the RMSE the proposed loss-based hyperprior leads to better results with respect to the benchmark prior in all the countries. The improvements are greater when we look at the average CRPS for every country from 1% for Argentina to 3% for India and Brazil.

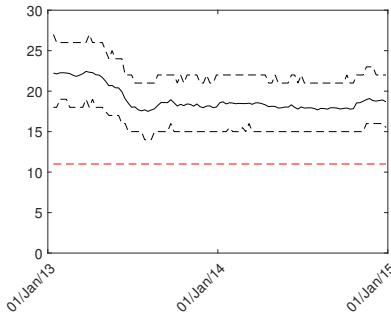


Figure 5: Estimated degrees of freedom (solid line) for the loss based hyperprior by using a rolling window of 104 weekly data with the 95% Highest posterior density (dotted lines) and the fixed ν (red dashed line) for the Dengue data.

	RMSE			CRPS		
	fixed ν	$\nu \sim \pi(\nu)$	ratio	fixed ν	$\nu \sim \pi(\nu)$	ratio
Argentina	0.328	0.329	1.002	0.174	0.172	0.992
Bolivia	0.228	0.227	0.993	0.145	0.144	0.989
Brazil	0.279	0.277	0.991	0.152	0.149	0.979
India	0.226	0.224	0.992	0.147	0.144	0.977
Indonesia	0.235	0.233	0.994	0.140	0.138	0.986
Mexico	0.273	0.271	0.994	0.150	0.148	0.989
Philippines	0.231	0.230	0.996	0.134	0.131	0.979
Singapore	0.687	0.685	0.997	0.326	0.323	0.991
Thailand	0.372	0.372	0.997	0.189	0.187	0.987
Venezuela	0.291	0.289	0.992	0.161	0.160	0.991

Table 4: RMSE and average CRPS for the Dengue Data for each prior. The first column refers to the variable, the second to the Gibbs sampler with fixed ν and the third with our loss-based hyperprior.

6 Discussions

We have presented a novel method to perform forecasting in Vector Autoregressive models (VAR), where a hyperprior is set on the number of degrees of freedom of the covariance matrix for the Normal-Wishart prior. In particular, the hyperprior considered can be considered objective, in the sense that it takes into considerations only the intrinsic properties of the model, i.e. sampling distribution plus the prior. The method has been compared with what is currently used in the literature, when no information about the parameter values of the Normal-Wishart prior is available, which is by setting $\nu = m + 1$.

The analysis of simulated data has shown that, when the true value of ν is close to $m + 1$, both approaches perform in a similar way. While, as one would expect, the farther the true ν is from $m + 1$, the better the performance of the proposed method. To illustrate in practice the advantage of having a loss-based prior on ν , we have analysed its performance in terms of prediction on two datasets. One concerns macroeconomic variable from the FRED dataset, and the other the analysis of dengue fever data. For both datasets it appears that the proposed method outperforms the one currently widely used, in particular when the CRPS index is considered.

In support of our results, we have estimated the number of degrees of freedom on rolling windows. This analysis has shown that the data contains information for a value of ν always above the value of $m + 1$, which justifies the use of the proposed method. In other words, as the data appear to have been “generated” by a Bayesian model with a relatively large number of degrees of freedom, by setting $\nu = m + 1$, one impacts on the predictive performance of the model. On the other hand, by assuming uncertainty of the value of ν , i.e. assigning an objective prior on it, the model is free to “choose” the most appropriate value of the parameter and, even considering the extra uncertainty that this implies, the results are better than the previous method.

References

Abramowitz, M. and Stegun, I. A. (1972). *Handbook of Mathematical Functions with Formulas, Graphs, and Mathematical Tables*. Dover, New York.

Ba  bura, M., Giannone, D., and Reichlin, L. (2010). Large bayesian vector auto regressions. *Journal of Applied Econometrics*, 25(1):71–92.

Billio, M., Casarin, R., and Rossini, L. (2019). Bayesian nonparametric sparse var models. *Journal of Econometrics*, 212(1):97–115.

Carneiro, H. A. and Mylonakis, E. (2009). Google trends: A web-based tool for real-time surveillance of disease outbreaks. *Clinical Infectious Diseases*, 49(10):1557–1564.

Carriero, A., Clark, T. E., , and Marcellino, M. (2015). Bayesian vars: Specification choices and forecast accuracy. *Journal of Applied Econometrics*, 30(1):46–73.

Carriero, A., Clark, T. E., and Marcellino, M. (2019). Large Bayesian vector autoregressions with stochastic volatility and non-conjugate priors. *Journal of Econometrics*, 212(1):137–154.

Cross, J. L., Hou, C., and Poon, A. (2020). Macroeconomic forecasting with large Bayesian VARs: Global-local priors and the illusion of sparsity. *International Journal of Forecasting*, 36(3):899–915.

Davis, R. A., Zang, P., and Zheng, T. (2016). Sparse vector autoregressive modeling. *Journal of Computational and Graphical Statistics*, 25(4):1077–1096.

Doan, T., Litterman, R., and Sims, C. (1984). Forecasting and conditional projection using realistic prior distributions. *Econometric Reviews*, 3(1):1–100.

Elezovic, N., Giordano, C., and Pecaric, J. (2000). The best bounds in gautschi’s inequality. *Math. Inequal. Appl.*, 3(2):239–252.

George, E. I., Sun, D., and Ni, S. (2008). Bayesian stochastic search for VAR model restrictions. *Journal of Econometrics*, 142(1):553–580.

Gneiting, T. and Raftery, A. E. (2007). Strictly proper scoring rules, prediction, and estimation. *Journal of the American statistical Association*, 102(477):359–378.

Gneiting, T. and Ranjan, R. (2011). Comparing density forecasts using threshold-and quantile-weighted scoring rules. *Journal of Business & Economic Statistics*, 29(3):411–422.

Huber, F. and Feldkircher, M. (2019). Adaptive shrinkage in bayesian vector autoregressive models. *Journal of Business & Economic Statistics*, 37(1):27–39.

Huber, F. and Rossini, L. (2020). Inference in bayesian additive vector autoregressive tree models. *arXiv preprint arXiv:2006.16333*.

Litterman, R. B. (1986). Forecasting with bayesian vector autoregressions – five years of experience. *Journal of Business & Economic Statistics*, 4(1):25–38.

McCracken, M. W. and Ng, S. (2020). Fred-qd: A quarterly database for macroeconomic research. *Federal Reserve Bank of St. Louis Review*.

Polgreen, P. M., Chen, Y., Pennock, D. M., Nelson, F. D., and Weinstein, R. A. (2008). Using internet searches for influenza surveillance. *Clinical Infectious Diseases*, 47(11):1443–1448.

Sims, C. A. (1980). Macroeconomics and reality. *Econometrica*, 48(1):1–48.

Sims, C. A. and Zha, T. (1998). Bayesian methods for dynamic multivariate models. *International Economic Review*, 39(4):949–968.

Strauss, R. A., Castro, J. S., Reintjes, R., and Torres, J. R. (2017). Google dengue trends: An indicator of epidemic behavior. the venezuelan case. *International Journal of Medical Informatics*, 104:26–30.

Villa, C. and Walker, S. G. (2015). An objective approach to prior mass functions for discrete parameter spaces. *Journal of the American Statistical Association*, 110(511):1072–1082.

A Further Simulation results

In this section, we have reported further simulation results. We have reported the Root mean absolute deviation (RMAD) for the case with $T = 100$. In particular, Figure A.1 shows the RMAD for the covariance matrix for the five dimensional case, when the data are generated from a Wishart distribution with degrees of freedom are equal to 5 (left); 10 (center) and 15 (right). The same arises in Figure A.2, where we have a ten dimensional case for the matrix of covariance and with data generated with 10 (left), 15 (center) and 20 (right) degrees of freedom. In conclusion, Figure A.3 shows the results for the twenty dimensional case, where the data are generated from a Wishart with 20 (left); 24 (center) and 26 (right) degrees of freedom.

As stated in the paper, the results shows improvements in the use of our loss-based prior with respect to a fixed ν prior when the data are generated with an higher than the dimension degrees of freedom.

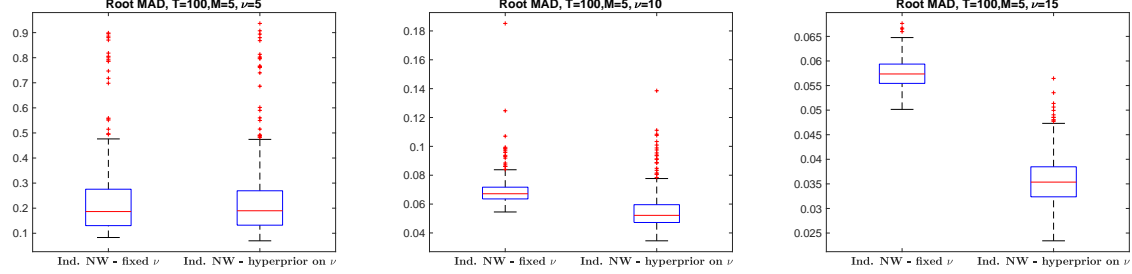


Figure A.1: Monte Carlo Simulation - Root Mean Absolute Deviations of the covariance matrices of dimension $m = 5$. These empirical distributions are obtained by simulating 250 VAR(1) of sample size $T = 100$. Results are reported separately for data generated from a Wishart with $\nu = 5$ (left panel); $\nu = 10$ (center panel) and $\nu = 15$ (right panel).

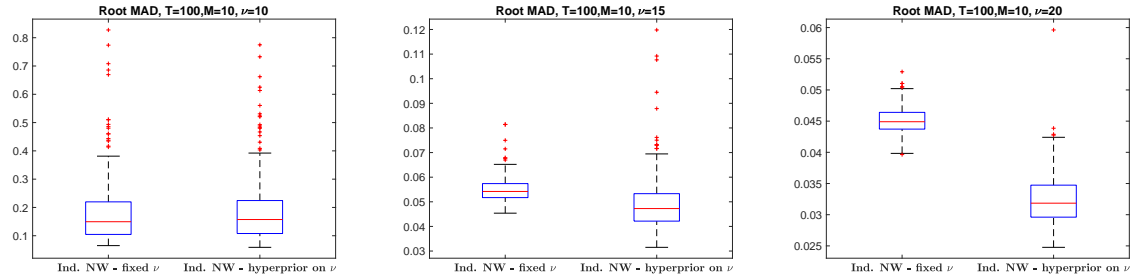


Figure A.2: Monte Carlo Simulation - Root Mean Absolute Deviations of the covariance matrices of dimension $m = 10$. These empirical distributions are obtained by simulating 250 VAR(1) of sample size $T = 100$. Results are reported separately for data generated from a Wishart with $\nu = 10$ (left panel); $\nu = 15$ (center panel) and $\nu = 20$ (right panel).

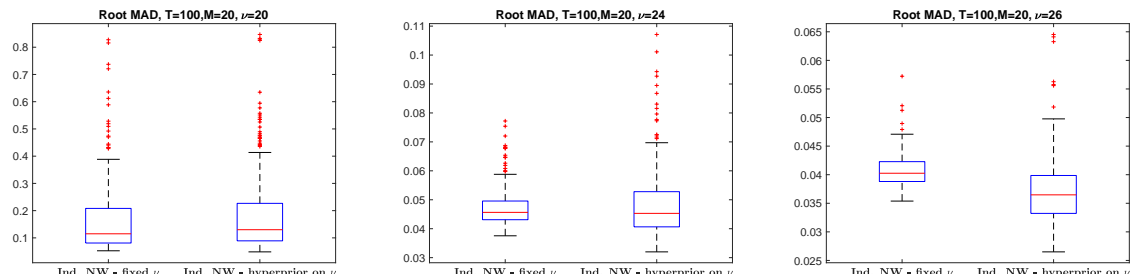


Figure A.3: Monte Carlo Simulation - Root Mean Absolute Deviations of the covariance matrices of dimension $m = 20$. These empirical distributions are obtained by simulating 250 VAR(1) of sample size $T = 100$. Results are reported separately for data generated from a Wishart with $\nu = 20$ (left panel); $\nu = 24$ (center panel) and $\nu = 26$ (right panel).